JOURNAL OF THEORETICAL AND APPLIED MECHANICS
52, 1, pp. 3-14, Warsaw 2014

THEORETICAL STUDY OF STRESS TRANSFER IN PLATELET REINFORCED COMPOSITES

A.M. Fattahi
Department of Mechanical Engineering, Tabriz Branch, Islamic Azad University, Tabriz, Iran
e-mail: a.fattahi@iaut.ac.ir.
M. Mondali
Department of Mechanical and Aerospace Engineering, Science and Research Branch, Islamic Azad University, Tehran, Iran

An analytical approach was developed for rectangular platelet reinforced composites which could be used for a 3D elastic stress field distribution subjected to an applied axial load. The ends of the platelet could be bonded to the matrix. Exact displacement solutions were derived for the matrix/platelet fromtheory of elasticity. These displacement solutions were then superposed for achieving analytical expressions for the matrix/platelet 3D stress field components over the entire composite system including the platelet end region, using the adding imaginary fiber technique. The platelet/matrix components could exactly satisfy the equilibrium and compatibility conditions and satisfy the equilibrium requirements and the overall boundary conditions. The obtained analytical results were then validated by FEM and Shear-lag modeling, and some of discrepancies among the shear-lag models were resolved. Good agreements were observed between the analytical and numerical predictions.

Key words: analytical modeling, platelet reinforced composites, stress transfer

1. Introduction

Over the past few decades, a variety of numerical and analytical models has been developed to investigate different stress transfer problems in composites. These models mainly include 1D models, which are typically based on the shear-lag theory (Agarwal, 1974; Agarwal and Broutman, 1980; Chang and Tarn, 2011; Cox, 1952; Glavinchevski and Piggott, 1973; Haque and Ramasetty, 2005; Hsueh, 1994, 2000; Hsueh *et al.*, 1999; Jiang and Peters, 2008; Jiang *et al.*, 1998; Kim, 1998, 2007, 2008; Kim and Kwac, 2009; Kim and Noh, 2004; Kotha *et al.*, 2000; Lusis *et al.*, 1973; Narin, 1997, 2004; Narin and Mendels, 2001; Padawer and Beecher, 1970; Piggott, 1980; Salekin *et al.*, 1992; Taya and Arsenault,1989; Tyson and Davies, 1965; Wu *et al.*, 1997), 3D analytical models based on axisymmetric analyses (Abedian *et al.*, 2007; Jiang *et al.*, 1998, 2004; Wu *et al.*, 1997), the Eshelby models based on Eshelby's equivalent inclusion method (Arsenault and Taya, 1987; Eshelby, 1957; Tanaka *et al.*, 1973; Lee, 2008; Withers *et al.*, 1989) and numerical models (Cannilloa *et al.*, 2003; Lusti *et al.*, 2002; Narin, 2007). Due to the complexity of elasticity field equations, analytical closed-form solutions to fully three-dimensional problems are very difficult to be obtained. Accordingly, many solutions have been developed for reduced problems that are typically composed of axisymmetry or one-dimensionality based on the shear-lag theory for simplifying a particular aspect of the formulation and solution. In mathematical terms, the shear-lag model is the simplest of all models, which is widely used for the stress transfer analysis in unidirectional composites. This model is based on a simple differential equation which relates the fibre axial stress to the interfacial shear stress. It is not applicable at higher volume fractions due to the significant interactions of fibres. Also, the model cannot predict changes of axial stress and strain distributions in the radial direction. As a result, due to these limitations, the shear-lag model cannot provide reliable predictions for the

composite properties, and thus, its application for short fibre composites has been limited over time. Most interfacial problems need the detailed distribution of stresses at the interface like the interface friction slip behavior in composites; however, the one-dimensional shear-lag model cannot provide this stress state. Three-dimensional analytical models have been developed based on quite different approaches and aim mostly at the interfacial problems. It has been noted that most of the three-dimensional analytical models usually satisfy the equilibrium states and most of the boundary and interfacial conditions. This is because the solutions are generally based on the stress equilibrium equations; but the compatibility conditions are only partly or approximately satisfied because of different degrees of applied approximations and simplifications. Therefore, since the excessive complicated mathematical derivations are involved, very limited efforts could be observed for the exact solution of such problems in the literature. One of the most precise and relatively simple three-dimensional analytical solutions was done by Jiang *et al.* (2004). In this model, two sets of exact displacement solutions for the matrix, i.e. the far-field solution and the transient solution, were derived. Afterwards, the theory of elasticity and superposition of the simplified analytical expressions were used to find all the stress components in the matrix and fibre. It is worth mentioning that the fibre end region could be also included using the imaginary fibre technique. Jiang's analytical model was modified and developed by Abedian *et al.* (2007). The latter was greatly improved and could predict capability of the composite behavior. In brief, for Jiang's and Abedian's models, the following assumptions were made: a perfect bond existed at the fibre-matrix interface and both fibre and matrix were isotropic.

Most authors have made emphasis on platelets as reinforcement instead of fibers because of their two-dimensional stiffening effects (Chou and Green, 1993; Piggott, 1980; Salekin *et al.*, 1992) and cost factor. The two-dimensional stress transfer model of platelet reinforced composites was presented by Tyson and Davis (1965), which was derived following the same analysis as applied in the classical shear-lag model by Cox (1952). Later, Hsueh (1994, 1999, 2000) proposed a more rigorous two-dimensional stress transfer model for platelet reinforcement while assuming that the shear stress in the matrix decreased linearly from the interface between the platelet and matrix to the edges. Also, the effects of matrix bonding at the ends, Young's modulus, and the aspect ratio of the platelet were investigated on stress transfer. A simple second order model and a more complicated fourth order model were developed for simulating stress transfer in overlapped platelets by Kotha *et al.* (2000). Some other models based on shear-lag theory were presented by Narin (1999, 2001, 2004).

The present study tried to derive such an analytical 3D modeling of platelet reinforced composites which were presented according to Jiang's and Abedian's methods and boundary conditions. While considering the typical complexity of stress field distribution in platelet reinforced composites, the analysis aimed at a platelet reinforced composite subjected to an applied axial load. Two sets of matrix/platelet displacement solutions, the far-field solution and the transient solution were precisely derived based on the theory of elasticity and were superposed to achieve simplified analytical expressions for the matrix/platelet stress field components and the platelet axial stress field components in the entire composite system, which included the platelet end region, using the technique of adding the imaginary fibre. The finite element numerical calculations were then conducted to examine the validity of this analytical model. At last, some concluding remarks were presented on the present analytical model. Both bonded and debonded platelet end cases were introduced in this research.

2. Analyses

2.1. Composite model

In the current study, a rectangular unit cell (as shown in Fig. 1) was used for modeling platelet reinforced composites. The platelet with the width of $2a$ and length of $2l$ was embedded in the

center of a matrix with the width of $2b$ and length of $2l'$. The area fraction and aspect ratio of the platelet were defined as follows $f = a/b$ and $s = l/a$, respectively. The axial stress (σ_0) was considered to be uniformly applied to the end faces of the unit cell. A Cartesian coordinate system (x, y) was also applied with its origin located in the centre of the unit cell, as given in Fig. 1. For simplicity, a perfect bond was assumed at the platelet/matrix interface and isotropic constituents for the composite. Due to the symmetric geometry in the x-y plane and boundary conditions, only one quarter of the unit cell was considered in the analysis. In this work, the solutions were performed in two separate areas: in the platelet region $(0 \leqslant y \leqslant l)$ and the platelet end region $(l \leqslant y \leqslant l')$. They were undertaken using the imaginary fibre technique (Abedian *et al.*, 2007; Jiang *et al.*, 2004), which assumed that the platelet end region was composed of an imaginary platelet surrounded with a rectangular matrix while the properties of the imaginary platelet were considered the same as those of the matrix.

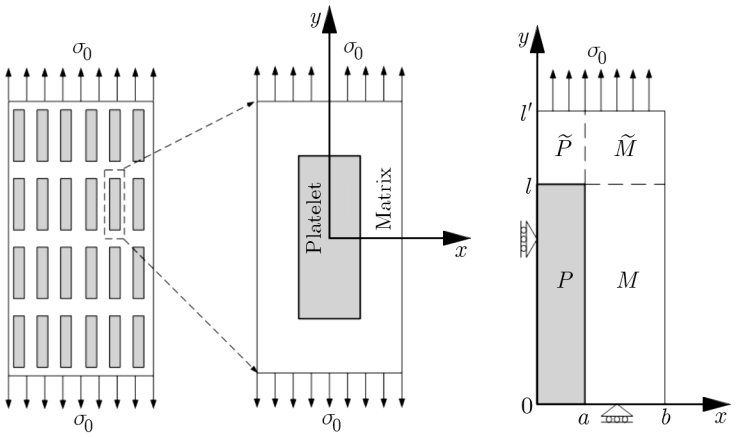

Fig. 1. Schematic illustrations of the unit cell

2.2. General solutions of matrix and platelet displacements

The equilibrium equations for plane stresses (Timoshenko and Goodier, 1951) are as follows

$$\frac{\partial \sigma_x}{\partial x} + \frac{\partial \tau_{xy}}{\partial y} = 0 \qquad \frac{\partial \sigma_y}{\partial y} + \frac{\partial \tau_{xy}}{\partial x} = 0 \tag{2.1}$$

which lead to the equations

$$\frac{2}{1+\nu}\frac{\partial^2 u}{\partial x^2} + \frac{1-\nu}{1+\nu}\frac{\partial^2 u}{\partial y^2} + \frac{\partial^2 w}{\partial x \partial y} = 0 \qquad \frac{1-\nu}{1+\nu}\frac{\partial^2 w}{\partial x^2} + \frac{2}{1+\nu}\frac{\partial^2 w}{\partial y^2} + \frac{\partial^2 u}{\partial x \partial y} = 0 \tag{2.2}$$

where u is the displacement in the x-direction, and w is the displacement in the y-direction, E s Young's modulus and ν is Poisson's ratio. By simple algebraic manipulation of the operators in Eqs. (2.1) and (2.2), the governing equations of w and u can be derived. The equation with respect to u could be found in the following manner

$$\frac{\partial^4 u}{\partial x^4} + 2\frac{\partial^4 u}{\partial x^2 \partial y^2} + \frac{\partial^4 u}{\partial y^4} = 0 \tag{2.3}$$

The method of separation variables verifies the last equation and results in different answers. For the case of this reserach, the Laplace equation could be obtained according to the conditions (see Appendix A). Thus, the following general solution can be found for the x-direction displacement

$$u^{m(T)}(x, y) = (A_1 \sin nx + A_2 \cos nx)(A_3 \sinh ny + A_4 \cosh ny) \tag{2.4}$$

where A_i $(i = 1 - 4)$ is an integral constant and n is a constant related to the eigenvalue. By substituting Eq. (2.4) into Eq. (2.1) or Eq. (2.2), the general solution for the y-direction displacement (w) can be derived as follows

$$w^{m(T)}(x,y) = (-A_1 \cos nx + A_2 \sin nx)(A_3 \cosh ny + A_4 \sinh ny) \tag{2.5}$$

Another set of the displacement general solutions for zero-eigenvalue were derived as demonstrated below (see Appendix A)

$$u^{m(0)}(x,y) = B_1 + B_2 x \qquad w^{m(0)}(x,y) = B_3 + B_4 y \tag{2.6}$$

where B_j $(j = 1, \ldots, 4)$ is the integral constant. The above displacement solutions could be superimposed to write the total value of displacement components in the matrix as follows

$$u^m = u^{m(0)} + u^{m(T)} \qquad w^m = w^{m(0)} + w^{m(T)} \tag{2.7}$$

The general solutions for the x- and y-directions displacements in the platelet could be found in Eqs. (2.8)-(2.10). It should be noted that, due to the continuity condition, $A_3$and A_4 were considered the same as those for the matrix expressions. But new boundary conditions were required for successful application in these equations, as presented in the next section. The details of derivation of the coefficients by the proposed boundary conditions will be also given in this investigation

$$\begin{aligned} u^{p(T)}(x,y) &= (A_5 \sin nx + A_6 \cos nx)(A_3 \sinh ny + A_4 \cosh ny) \\ w^{p(T)}(x,y) &= (-A_5 \cos nx + A_6 \sin nx)(A_3 \cosh ny + A_4 \sinh ny) \end{aligned} \tag{2.8}$$

and

$$u^{p(0)}(x,y) = B_5 + B_6 x \qquad w^{p(0)}(x,y) = B_7 + B_8 y \tag{2.9}$$

and

$$u^p = u^{p(0)} + u^{p(T)} \qquad w^p = w^{p(0)} + w^{p(T)} \tag{2.10}$$

Thus, the general solutions for the stress and strain components which correspond to the above two sets of displacement solutions were obtained using Hook's law (see Appendix B). Therefore, the stress field described by displacement Eqs. (2.6) and (2.9) was identical to the one in a composite with infinitely long platelets which were subjected to a far-field load corresponding to the uniform portion of the total stress. However, the stress field described by Eqs. (2.4), (2.5), and (2.8) corresponded to the non-uniform portion of the total stress field since all the components of the stress field depended on both x- and y-directions.

3. Solution for platelet

3.1. Far-field solution

The surface conditions for the far-field solution in the platelet region for the platelet bonded end case could be presented by

$$\tau_{xy}^{m(0)}(b,y) = 0 \qquad w^{m(0)}(x,0) = 0 \qquad u^{p(0)}(0,y) = 0 \tag{3.1}$$

The above conditions and $\varepsilon_{yy}^{m(0)} = \varepsilon_0$ can be used for deriving the following constants

$$B_3 = B_5 = 0 \qquad B_4 = \varepsilon_0 \tag{3.2}$$

where ε_0 is the far-field strain. Using Eq. (B.7), other constants could be found as demonstrated below

$$B_8 = \varepsilon_0 \tag{3.3}$$

Using $u^{m(0)}(a,y) = u^{p(0)}(a,y)$, the B_1 coefficient can be obtained as follows

$$B_1 = (B_6 - B_2)a \tag{3.4}$$

Equation (B.8) and the equation of the equilibrium, i.e. Eq. $(3.5)_1$, lead to obtaining B_2 and B_6 as in Eqs. $(3.5)_{2,3}$

$$\sigma_0 = f\overline{\sigma}_{yy}^{p(0)} + (1-f)\overline{\sigma}_{yy}^{m(0)} \qquad B_2 = p_{21}\sigma_0 + p_{22}\varepsilon_0 \qquad B_6 = p_{61}\sigma_0 + p_{62}\varepsilon_0 \tag{3.5}$$

Also, p_{21}, p_{22}, p_{61} and p_{62} were found in Matlab software. Due to being so lengthy, they were not cited in this paper.

Then, the stresses in the imaginary platelet region $(l \leqslant y \leqslant l')$ were calculated. Similarly, the far-field solution and all the corresponding expressions of the general solution for the stress and strain components of this region could be obtained directly from those of the platelet region by considering $E_p = E_m$ and $\nu_p = \nu_m$. Using the same derivation procedures as the ones in the platelet region, the integral constants in this region were obtained

$$\begin{aligned} &\widetilde{B}_1 = \widetilde{B}_5 = 0 && \widetilde{B}_4 = \widetilde{B}_8 = \widetilde{\varepsilon}_0 \\ &\widetilde{B}_3 = \widetilde{B}_7 = (\varepsilon_0 - \widetilde{\varepsilon}_0)l && \widetilde{B}_2 = \widetilde{B}_6 = \frac{(1-\nu_m^2)\sigma_0 - E_m\widetilde{\varepsilon}_0}{\nu_m E_m} \end{aligned} \tag{3.6}$$

To calculate the far-field strains ε_0 and $\widetilde{\varepsilon}_0$, the following two boundary conditions could be used

$$u^{m(0)}(b,y) = \widetilde{u}^{m(0)}(b,y) \qquad \frac{l}{l'}[fE_p + (1-f)E_m]\varepsilon_0 + \Big(1 - \frac{l}{l'}\Big)E_m\widetilde{\varepsilon}_0 = \sigma_0 \tag{3.7}$$

Here, Matlab software was used to find ε_0 and $\widetilde{\varepsilon}_0$ strains. Because of being lengthy, they were not cited in this paper. Equation $(3.7)_2$ can be obtained from the boundary conditions and some simplifications which lead to having l and l' inside the strain equations, equilibrium equations

$$\begin{aligned} &\frac{l}{l'}\sigma_0 + \Big(1 - \frac{l}{l'}\Big)\sigma_0 = \sigma_0 && \sigma_0 = f\sigma_{yy}^{p(0)} + (1-f)\sigma_{yy}^{m(0)} \\ &\sigma_0 = f\widetilde{\sigma}_{yy}^{p(0)} + (1-f)\widetilde{\sigma}_{yy}^{m(0)} && \sigma_{yy}^{m(0)} = E_m\varepsilon_0 \\ &\sigma_{yy}^{p(0)} = E_p\varepsilon_0 && \widetilde{\sigma}_{yy}^{m(0)} = \widetilde{\sigma}_{yy}^{p(0)} = E_m\widetilde{\varepsilon}_0 \end{aligned} \tag{3.8}$$

Finally, by substituting ε_0 and $\widetilde{\varepsilon}_0$ and the above-obtained constants in the stress equations, the expressions for the far-field solutions in the two mentioned regions can be found as a function of σ_0.

3.2. Transient solution

In this part, the transient solution in the platelet region $(0 \leqslant y \leqslant l)$ will be first determined. The surface boundary conditions for the transient solution can be presented by

$$w^{m(T)}(x,0) = 0 \qquad u^{m(T)}(b,y) = 0 \tag{3.9}$$

It is implied by these conditions that the transient solution did not alter the shape of the unit cell. Substituting the above conditions in the stress, the strain and displacement expressions resulted in

$$A_3 = 0 \qquad A_2 = -A_1 \tan nb \tag{3.10}$$

To determine two other coefficients, the following boundary conditions were used

$$u^{p(T)}(0,y)=0 \qquad \sigma_{xx}^{m(T)}(a,y)=\sigma_{xx}^{p(T)}(a,y) \tag{3.11}$$

Then, A_5 and A_6 were derived

$$A_6=0 \qquad A_5=\frac{E_m}{E_p}\frac{1+\nu_p}{1+\nu_m}(A_1-A_2\tan na) \tag{3.12}$$

To find the unknown n, axial force equilibrium Eq. (3.13) was used. Matlab software was used for finding the optimum n

$$f\overline{\sigma}_{yy}^{p(T)}+(1-f)\overline{\sigma}_{yy}^{m(T)}=0 \tag{3.13}$$

Afterwards, the transient solution was specified in the platelet end region $(l\leqslant y\leqslant l')$. The transient solution and all the corresponding expressions for the general solution of the stress and strain components in this region could be directly obtained from those of the platelet region by considering $E_p=E_m$ and $\nu_p=\nu_m$. Using the same derivation procedure and corresponding boundary conditions as the ones in the platelet region, the corresponding constants were achieved as follows

$$\widetilde{\tau}_{xy}^{m(T)}(b,y)=0 \qquad \widetilde{w}^{m(T)}(a,y)=\widetilde{w}^{p(T)}(a,y) \qquad \widetilde{\sigma}_{xx}^{m(T)}(a,y)=\widetilde{\sigma}_{xx}^{p(T)}(a,y) \tag{3.14}$$

Also, the following constants were obtained

$$\widetilde{A}_6=0 \qquad \widetilde{A}_5=\widetilde{A}_1-\widetilde{A}_2\tan\widetilde{n}a \qquad \widetilde{A}_2=-\widetilde{A}_1\tan\widetilde{n}b \tag{3.15}$$

To find the unknown $\widetilde{n}$, equilibrium Eq. (3.16) was used, similar to the real platelet field

$$f\overline{\widetilde{\sigma}}_{yy}^{p(T)}+(1-f)\overline{\widetilde{\sigma}}_{yy}^{m(T)}=0 \tag{3.16}$$

Using the following surface condition, Eq. $(3.17)_1$, $\widetilde{A}_3$ coefficient was also derived

$$\widetilde{\tau}_{xy}^{m}(x,l')=\widetilde{\tau}_{xy}^{p}(x,l')=0 \qquad \widetilde{A}_3=-\widetilde{A}_4\frac{\sinh\widetilde{n}l'}{\cosh\widetilde{n}l'} \tag{3.17}$$

Finally, A_4 and $\widetilde{A}_4$ coefficients were found using the following boundary conditions

$$\overline{\sigma}_{yy}^{p}(x,l)=\overline{\widetilde{\sigma}}_{yy}^{p}(x,l) \qquad \tau_{xy}^{m}(a,y)=\widetilde{\tau}_{xy}^{m}(a,y) \tag{3.18}$$

4. Analytical and numerical predictions

To monitor the validity of the current analytical model, a comparison was made with the FEM calculations by ANSYS software. The schematic FEM model is also demonstrated in Fig. 1. The numerical calculations were performed on one quarter of the unit cell due to the existing symmetric boundary conditions. Eight nodded PLANE82 solid elements were applied for the purpose of meshing. Loading in ANSYS was via pressure applied to the element boundary line. All the simulations were performed under the plane stress condition. The boundary conditions required fixing both the x-displacement at $x=0$ and the y-displacement at $y=0$. The loading was applied to $y=l'$. Only typical results were presented for $b/a=1.75$, $l/a=5$ and $l/l'=0.5$ (platelet volume fraction was almost 0.285) in order to decrease the number of figures. The material properties were selected as $E_m=63\,\mathrm{GPa}$, $E_p=402\,\mathrm{GPa}$, $\nu_m=0.22$ and $\nu_p=0.23$ (Cannilloa *et al.*, 2003). The applied stress was taken as $\sigma_0=200\,\mathrm{MPa}$.

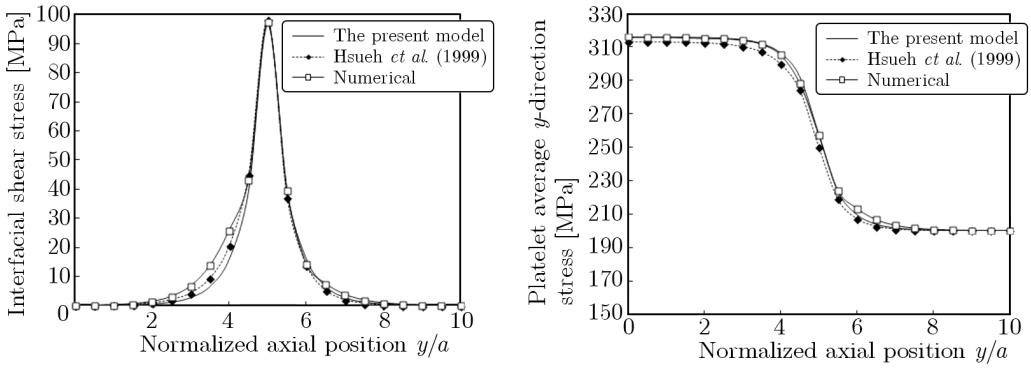

Fig. 2. Comparison and validation of the present model with Hsueh's model and numerical results

Figure 2 demonstrates the comparison and validation of the present model with the Hsueh model and its numerical results. Compared with Hsueh's results, the current model and FEM values of the stress components for the case of perfect bond were found to be in a good agreement.

To demonstrate the capabilities of the present model, displacements, strains, stresses in the matrix and platelet were given in the x- and y-directions. It is worth considering that only typical results were presented in order to reduce the number of figures. The analytical and numerical curves of the normalized matrix in displacements in the x- and y-directions on the outer surface of the unit cell and the platelet/matrix interface versus the normalized axial position are demonstrated in Fig. 3. As can be observed, considerable agreements were obtained between the analytical and numerical predictions. Figure 4 depicts the analytical and numerical curves of the shear stress and x-direction stresses on the outer surface of the unit cell $(x = b)$ and the platelet-matrix interface versus the normalized axial position y/a.

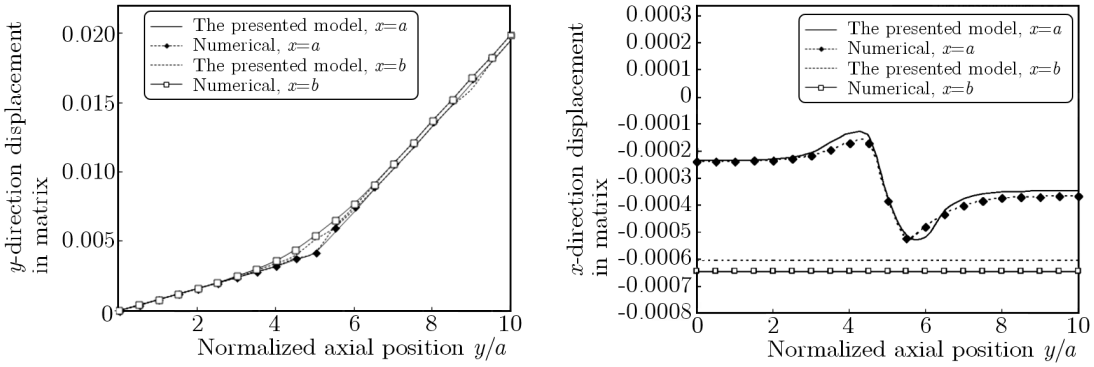

Fig. 3. Analytical and numerical curves of the matrix displacements vs. the normalized axial position

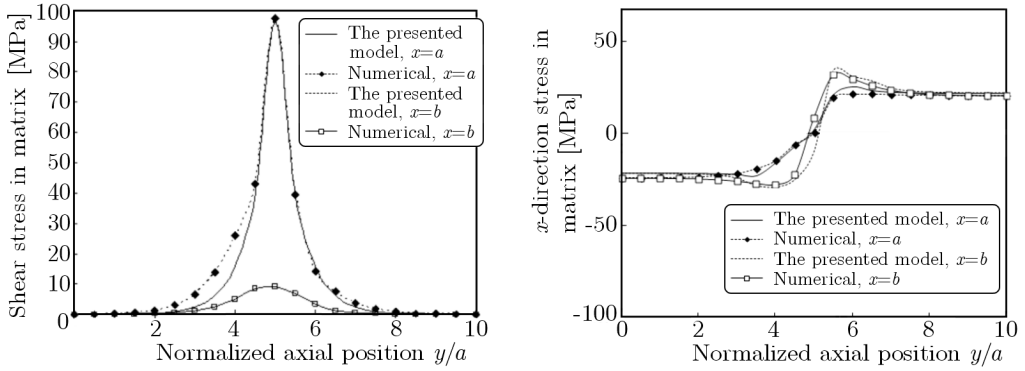

Fig. 4. Analytical and numerical curves of the matrix stress vs. the normalized axial position

The given comparisons confirmed considerable strong prediction ability of the analytical solution for the elastic field distribution in such a complicated system. There are some small inconsistencies in singular behavior on the platelet end plane between the analytical and numerical solutions, which can be probably attributed to the limited prediction ability of the finite element numerical method for the stress singularity. These calculations also demonstrated that the same consistent predictions could be achieved for all the strain components and over a great range of material properties and geometries, which were not included here.

5. Conclusions

An analytical model was developed for the analysis of the 3D elastic stress field in a platelet reinforced composite subjected to an axial load. The present stress field solution involved two regions, i.e. the matrix region surrounding the platelet and the platelet region. The derived analytical expressions for the matrix and platelet stress fields precisely satisfied both equilibrium and compatibility conditions of the theory of elasticity. Furthermore, since the interface continuity conditions and axial force equilibrium conditions were taken into account, the overall equilibrium was ensured rigorously within the platelet, matrix and between the platelet and the matrix.

Apart from the investigations based on the shear-lag theory, the stress transfer from the matrix to the platelet was obtained through the interface continuity conditions and the axial force equilibrium conditions. Furthermore, this model of the platelet reinforced composite presented all stress, strain and displacement components in the matrix and platelet; in contrast, shear-lag model only could predict the y-direction average stress in the platelet and the interface shear stress.

Because the number of boundary conditions, equilibrium and compatibility conditions was more than the number of unknown coefficients $(A_j,\, B_j,\, n,\, \widetilde{n})$, optimization methods were used for finding the best answers.

A. Solution for matrix displacements

$$\frac{\partial^2 u}{\partial x^2} + \frac{\partial^2 u}{\partial y^2} = 0 \tag{A.1}$$

Using the method of separation of variables for writting $u(x,y)$ as

$$u(x,y) = Y(y)X(x) \tag{A.2}$$

substitution of $u(x,y)$ into Eq. (A.1) leads to

$$\frac{\partial^2 X}{\partial x^2} + nX = 0 \qquad \frac{\partial^2 Y}{\partial x^2} - nY = 0 \tag{A.3}$$

Then, the following can be given

$$X = A_1 \sin nx + A_2 \cos nx \qquad Y = A_3 \sinh ny + A_4 \cosh ny \tag{A.4}$$

So

$$u^{m(T)}(x,y) = (A_1 \sin nx + A_2 \cos nx)(A_3 \sinh ny + A_4 \cosh ny) \tag{A.5}$$

For the far-field case $n = 0$, then

$$X^{m(0)} = B_1 + B_2 x \qquad Y^{m(0)} = C_1 + C_2 y \tag{A.6}$$

So

$$u^{m(0)}(x,y) = (B_1 + B_2 x)(C_1 + C_2 y) \tag{A.7}$$

where B_1, B_2, C_1 and C_2 are constants. The boundary conditions can be used with some simplifications, which results in

$$u^{m(0)}(x,y) = B_1 + B_2 x \tag{A.8}$$

Substitution of elements of Eqs. (A.5), (A.8) into Eq. (2.1) leads to

$$\begin{aligned} &w^{m(T)}(x,y) = (-A_1 \cos nx + A_2 \sin nx)(A_3 \cosh ny + A_4 \sinh ny) \\ &w^{m(0)}(x,y) = B_3 + B_4 y \end{aligned} \tag{A.9}$$

B. Boundary conditions

$$\begin{aligned} &u^m(b,y) = \widetilde{u}^m(b,y) && \tau^m_{xy}(b,y) = \widetilde{\tau}^m_{xy}(b,y) = 0 \\ &w^m(x,0) = w^p(x,0) = 0 && \tau^m_{xy}(x,0) = \tau^p_{xy}(x,0) = 0 \\ &\widetilde{w}^m(x,l') = \widetilde{w}^p(x,l') && \widetilde{\tau}^m_{xy}(x,l') = \widetilde{\tau}^p_{xy}(x,l') = 0 \end{aligned} \tag{B.1}$$

The interface continuity conditions on the platelet-matrix interface $(x = a)$

$$\begin{aligned} &\varepsilon^m(a,y) = \varepsilon^p(a,y) && \sigma^m_{xx}(a,y) = \sigma^p_{xx}(a,y) \\ &\widetilde{\varepsilon}^m(a,y) = \widetilde{\varepsilon}^p(a,y) && \widetilde{\sigma}^m_{xx}(a,y) = \widetilde{\sigma}^p_{xx}(a,y) \end{aligned} \tag{B.2}$$

The continuity conditions on the platelet end surface $(x = l)$

$$\begin{aligned} &\overline{\sigma}^m_{yy}(x,l) = \overline{\widetilde{\sigma}}^m_{yy}(x,l) && \overline{\sigma}^p_{yy}(x,l) = \overline{\widetilde{\sigma}}^p_{yy}(x,l) \\ &\tau^m_{yy}(x,l) = \widetilde{\tau}^m_{yy}(x,l) && w^m(x,l) = \widetilde{w}^m(x,l) \end{aligned} \tag{B.3}$$

C. General solutions for the stress and strain components

According to the theory of elasticity, the elastic constituent relations could be written as follows

$$\begin{aligned} &\tau_{xy} = \tau_{yx} = \frac{E}{2(1-\nu)}\gamma_{xy} && \sigma_{xx} = \frac{E}{1-\nu^2}(\varepsilon_{xx} + \nu\varepsilon_{yy}) \\ &\sigma_{yy} = \frac{E}{1-\nu^2}(\nu\varepsilon_{xx} + \varepsilon_{yy}) && \varepsilon_{xx} = \frac{\partial u}{\partial x} \\ &\varepsilon_{yy} = \frac{\partial w}{\partial y} && \gamma_{xy} = \gamma_{yx} = \frac{\partial u}{\partial y} + \frac{\partial w}{\partial x} \end{aligned} \tag{C.1}$$

where σ, ε, τ and γ are the normal stress and strain and the shear stress and strain, respectively. The following equations present the far-field solution of the matrix. Note that, for the end fiber region; i.e. $l \leqslant y \leqslant l'$, all the coefficients should have the tilde

$$\begin{aligned} &\sigma^{m(0)}_{xx}(x,y) = \frac{E_m}{1-\nu_m^2}(B_2 + \nu_m B_4) && \sigma^{m(0)}_{yy}(x,y) = \frac{E_m}{1-\nu_m^2}(\nu_m B_2 + B_4) \\ &\tau^{m(0)}_{xy}(x,y) = 0 && \varepsilon^{m(0)}_{xx}(x,y) = B_2 \\ &\varepsilon^{m(0)}_{yy}(x,y) = B_4 && \gamma^{m(0)}_{xy}(x,y) = \gamma^{m(0)}_{yx} = 0 \end{aligned} \tag{C.2}$$

The far-field solution for the fiber and imaginary fiber regions will be shown as follows. It is worth considering that, for the imaginary fiber, E_p and ν_p should be converted to E_m and ν_m, and all the coefficients should have the tilde

$$\begin{aligned}
&\sigma_{xx}^{p(0)}(x,y) = \frac{E_p}{1-\nu_p^2}(B_6 + \nu_p B_8) && \sigma_{y}^{p(0)}(x,y) = \frac{E_p}{1-\nu_p^2}(B_8 + \nu_p B_6)\\
&\tau_{xy}^{p(0)}(x,y) = 0 && \varepsilon_{xx}^{p(0)}(x,y) = B_6\\
&\varepsilon_{yy}^{p(0)}(x,y) = B_8 && \gamma_{xy}^{p(0)}(x,y) = \gamma_{yx}^{p(0)}(x,y) = 0
\end{aligned} \tag{C.3}$$

The transient solution of the matrix is given below. For the end platelet region; i.e. $l \leqslant y \leqslant l'$, all the coefficients should have the tilde

$$\begin{aligned}
\sigma_{xx}^{m(T)}(x,y) &= \frac{nE_m}{1+\nu_m}(A_1\cos nx - A_2\sin nx)(A_3\sinh ny + A_4\cosh ny)\\
\sigma_{yy}^{m(T)}(x,y) &= \frac{nE_m}{1+\nu_m}(-A_1\cos nx + A_2\sin nx)(A_3\sinh ny + A_4\cosh ny)\\
\tau_{xy}^{m(T)}(x,y) &= \frac{nE_m}{1+\nu_m}(A_1\sin nx + A_2\cos nx)(A_3\cosh ny + A_4\sinh ny)\\
\varepsilon_{xx}^{m(T)}(x,y) &= n(A_1\cos nx - A_2\sin nx)(A_3\sinh ny + A_4\cosh ny)\\
\varepsilon_{yy}^{m(T)}(x,y) &= n(-A_1\cos nx + A_2\sin nx)(A_3\sinh ny + A_4\cosh ny)\\
\gamma_{xy}^{m(T)}(x,y) &= 2n(A_1\sin nx + A_2\cos nx)(A_3\cosh ny + A_4\sinh ny)
\end{aligned} \tag{C.4}$$

For the transient solution of the platelet and imaginary platelet, one may reach the following equations. For the imaginary platelet, the E_p and ν_p should be converted to E_m and ν_m, and all the coefficients should have the tilde

$$\begin{aligned}
\sigma_{xx}^{p(T)}(x,y) &= \frac{nE_p}{1+\nu_p}(A_5\cos nx - A_6\sin nx)(A_3\sinh ny + A_4\cosh ny)\\
\sigma_{yy}^{p(T)}(x,y) &= \frac{nE_p}{1+\nu_p}(-A_5\cos nx + A_6\sin nx)(A_3\sinh ny + A_4\cosh ny)\\
\tau_{xy}^{p(T)}(x,y) &= \frac{nE_p}{1+\nu_p}(A_5\sin nx + A_6\cos nx)(A_3\cosh ny + A_4\sinh ny)\\
\varepsilon_{xx}^{p(T)}(x,y) &= n(A_5\cos nx - A_6\sin nx)(A_3\sinh ny + A_4\cosh ny)\\
\varepsilon_{yy}^{p(T)}(x,y) &= n(-A_5\cos nx + A_6\sin nx)(A_3\sinh ny + A_4\cosh ny)\\
\gamma_{xy}^{p(T)}(x,y) &= 2n(A_5\sin nx + A_6\cos nx)(A_3\cosh ny + A_4\sinh ny)
\end{aligned} \tag{C.5}$$

References

1. Abedian A., Mondali M., Pahlavanpour M., 2007, Basic modifications in 3D micromechanical modeling of short fibre composites with bonded and debonded fibre end, *Computational Materials Science*, **40**, 421-433
2. Agarwal B.D., Broutman L.J., 1980, *Analysis and Performance of Fibre Composites*, John Wiley and Sons, New York
3. Agarwal B.D., Lifsitz J.M., Broutman L.J., 1974, Elastic plastic finite element analysis of short fibre composites, *Fibre Science and Technology*, **7**, 45-62
4. Arsenault R.J., Taya M., 1987, Thermal residual stress in metal matrix composite, *Acta Metallurgica*, **35**, 651-659

5. Cannilloa V., Pellacania G.C., Leonelli C., Boccaccini A.R., 2003, Numerical modelling of the fracture behaviour of a glass matrix composite reinforced with alumina platelets, *Composites, Part A*, **34**, 43-51
6. Chang H.H., Tarn J.-Q., 2011, Three-dimensional elasticity solutions for rectangular orthotropic plates, *Journal of Elasticity*, **97**, 131-154
7. Cox H.L., 1952, The elasticity and strength of paper and other fibrous mterials, *British Journal of Applied Physics*,**3**, 72-79
8. Eshelby J.D., 1957, The determination of the elastic field of an ellipsoidal inclusion and related problems, *Proceedings of the Royal Society*, **A 241**, 376-396
9. Glavinchevski B., Piggott M., 1973, Steel disc reinforced polycarbonate, *Journal of Materials Science*, **8**, 1373-1382
10. Jiang G., Peters K., 2008, A shear-lag model for three-dimensional, unidirectional multilayered structures, *International Journal of Solids and Structures*, **45**, 4049-4067
11. Hsueh C.H., 1994, A two-dimentional stress transfer model for platelet reinfocement, *Composites Part B: Engineering*, **4**, 10, 1033-1043
12. Hsueh C.H., 2000, Young's modulus of unidirectional discontinuous-fibre composites, *Composites Science and Technology*, **60**, 2671-2680
13. Hsueh C.H., Fuller E.R., Langer S.A., Carter W.C., 1999, Analytical and numerical analyses for two-dimensional stress transfer, *Materials Science and Engineering*, **A268**, 1-7
14. Haque A., Ramasetty A., 2005, Theoretical study of stress transfer in carbon nanotube reinforced polymer matrix composites, *Composite Structures*, **71**, 68-77
15. Jiang Z., Lian J., Yang D., Dong S., 1998, An analytical study of the influence of thermal residual stresses on the elastic and yield behaviors of short fibre-reinforced metal matrix composites, *Materials Science and Engineering*, **A248**, 256-275
16. Jiang Z., Liu X., Li G., Lian J., 2004, A new analytical model for three-dimensional elastic stress field distribution in short fibre composite, *Materials Science and Engineering*, **A366**, 381-396
17. Kim H.G., Noh H.G., 2004, Effects of elastic modulus ratio on internal stresses in short fibre composites, *Journal of the Korean Society of Machine Tool Engineers*, **13**, 4, 73-78
18. Kim H.G., Kwac L.K., 2009, Evaluation of elastic modulus for unidirectionally aligned short fibre composites, *Journal of Mechanical Science and Technology*, **23**, 54-63
19. Kim H.G., 1998, Analytical study on the elastic-plastic transition in short fibre reinforced composites, *KSME International Journal*, **12**, 2, 257-266
20. Kim H.G., 2007, Investigation of stress field evaluated by elastic-plastic analysis in discontinuous composites, *International Journal of Automobile Technology*, **8**, 4, 483-491
21. Kim H.G., 2008, Effects of fibre aspect ratio evaluated by elastic analysis in discontinuous composites, *Journal of Mechanical Science and Technology*, **22**, 411-419
22. Kotha S.P., Kotha S., Guzelsu N., 2000, A shear-lag model to account for interaction effects between inclusions in composites reinforced with rectangular platelets, *Composites Science and Technology*, **60**, 2147-2158
23. Lee J.K., 2008, A study on validity of using average fibre aspect ratio for mechanical properties of aligned short fibre composites with different fibre aspect ratios, *Archive of Applied Mechanics*, **78**, 1-9
24. Liu G., Ji B., Hwang K.C., Khoo B.C., 2011, Analytical solutions of the displacement and stress fields of the nanocomposite structure of biological materials, *Composites Science and Technology*, **71**, 1190-1195
25. Lusis J., Woodhams R.T., Xanthos M., 1973, The effect of flake aspect ratio on the flexural properties of mica reinforced plastics, *Polymer Engineering and Science*, **13**, 2, 139-145

26. Lusti H.R., Hine P.J., Gusev A.A., 2002, Direct numerical predictions for the elastic and thermoelastic properties of short fibre composites, *Composites Science and Technology*, **62**, 1927-1934

27. Nairn J.A., 2007, Numerical implementation of imperfect interfaces, *Computational Materials Science*, **40**, 525-536

28. Narin J.A., Mendels D.A., 2001, On the use of planar shear-lag methods for stress-transfer analysis of multilayered composites, *Mechanics of Matrials*, **33**, 335-362

29. Narin J.A., 1997, On the use of shear-lag methods for analysis of stress transfer in unidirectional composites, *Mechanics of Matrials*, **26**, 63-80

30. Narin J.A., 2004, Generalized shear-lag analysis including imperfect interfaces, *Adv. Comp. Letts.*, **13**, 263-274

31. Padawer G.E., Beecher N., 1970, On the strength and stifness of planar reinforced plastic resins, *Polymer Engineering and Science*, **10**, 3, 185-192

32. Piggott M.R., 1980, In: *Load Bearing Fiber Composites*, Pergamon Press, Elmsford, NY, 141

33. Salekin S., Haque A., Huq N., Copes J.S., Mahfuz H., Jeelani S., 1992, Effect of reinforcement geometry on the mechanical properties of SiC/Al2O3 composites, *Composites*, **2**, 4, 242-259

34. Tanaka T., Wakashima K., Mori T., 1973, Plastic deformation anisotropy and work-hardening of composite materials, *Journal of the Mechanics and Physics of Solids*, **21**, 207-214

35. Taya M., Arsenault R.J., 1989, *Metal Matrix Composites Thermomechanical Behavior*, Pergamon Press, USA

36. Timoshenko S., Goodier J.N., 1951, *Theory of Elasticity*, New York, Toronto, London, McGraw-Hill Book Comp.

37. Tyson W.R., Davies G.J., 1965, A photoelastic study of the shear stresses associated with the transfer of stress during fibre reinforcement, *British Journal of Applied Physics*,**16**,199

38. Withers P.J., Stobss W.M., Pedersen O.B., 1989, The application of the Eshelby method of internal stress determination to short fibre metal matrix composites, *Acta Metallurgica*, **37**, 3061-3084

39. Wu W., Desaeger M., Verpoest I., Varna J., 1997, An improved analysis of the stresses in a single-fibre fragmentation test: I. Two-phase model, *Composites Science and Technology*, **57**, 809-819

40. Wu W., Verpoest I., Varna J., 1998, An improved analysis of the stresses in a single-fibre fragmentation test: II. 3-phase model, *Composites Science and Technology*, **58**, 41-50

Manuscript received February 15, 2013; accepted for print April 15, 2013